The structure of the critical layer of a swirling annular flow in transition

Jeanette Hussong, Nikolaus Bleier and Venkatesa Iyengar Vasanta Ram

July 10, 2006

Institut für Thermo- und Fluiddynamik
Ruhr Universität Bochum
44780 Bochum, Germany
vvr@lstm.ruhr-uni-bochum.de

1 Introduction

Swirl in a flow is a feature commonly met with in a wide variety of flows both in nature and in engineering. We use this term here to denote flows characterised by helical streamlines. Two transition mechanisms with some fundamental differences, which we call here the Taylor and the Tollmien-Schlichting mechanisms, stand generally in competition with each other in this flow. The salient difference between these two mechanisms is the presence or otherwise of a *critical layer*. The Tollmien-Schlichting mechanism exhibits a *critical layer*, whereas no such layer exists in the Taylor mechanism. Physically, the *critical layer* is the region within the shear layer in which effects of viscosity are crucial to the dynamics of disturbances influencing transition, and so cannot be ignored in the study of propagation characteristics of disturbances in the context of transition. Mathematically, the *critical layer* occurs at a location where the differential equations governing the disturbances exhibit a *turning point*, or, in other words, where the coefficient of the second derivative of the velocity passes through a zero. For a more complete discussion of the role of viscosity in the critical layer during transition and for a treatment of singular perturbation problems involving a turning point the reader is referred to literature on this subject, for example, [1, 2, 3, 4, 5, 7, 8, 9, 12].

The flow geometry we propose to study in this paper is the swirling annular flow in the gap between concentric circular cylinders. Swirl may be

brought about in this flow by an axial pressure gradient acting simultaneously with rotation of one or both the cylinders about its own axis. Further imposition of an axial motion on the cylinder walls results in a redistribution of the axial velocity profile, but which retains the basic qualitative character sought in the flow under study, viz. helical streamlines. The rotation of one or both of the cylinders and the axial movement of the walls together with an axial pressure gradient defines a class of flows subject to the two mechanisms of transition mentioned earlier. A judicial choice of a relativey small number of parameters permits the axial and azimuthal velocity profiles in the class of flows thus generated to exhibit a wide variety of distributions in which the two transition mechanisms can interact with each other to yield flows with different topological characteristics, and hence its suitability for our present study. However, we restrict our attention in this paper to flows generated by rotation of the outer cylinder alone, and axial motion of the inner cylinder alone. We note that both these conditions tend to stabilise the flow. Our focus of interest in this paper is the location and structure of the *critical layer* that appears in this flow when it is undergoing transition.

2 Formulation of the problem

The flow geometry is sketched in Fig.1 which also serves to explain some of the notations. The parameters in the problem are: the radii of the outer and inner cylinders, R_a and R_i respectively, the axial pressure gradient $\frac{dP_G}{dx}$, or the reference velocity $V_{ref_{xp}}$ derivable herefrom through $V_{ref_{xp}} = -\frac{H^2}{2\mu}\frac{dP_G}{dx}$, the angular velocity of the outer cylinder Ω_a, the axial velocity of inner cylinder $V_{ref_{xwi}}$ and the kinematic viscosity ν. The dimensionless parameters in the problem are then: the transverse curvature parameter $\epsilon_R = \frac{R_a - R_i}{R_a + R_i}$, the Reynolds number $Re = \frac{V_{ref_{xp}} H}{\nu}$ referred to $V_{ref_{xp}}$ and the semi-gap width $H = \frac{(R_a - R_i)}{2}$, the swirl parameter $S_{wa} = \frac{\Omega_a R_a}{V_{ref_{xp}}}$ and the translation velocity parameter $T_{wi} = \frac{V_{refxwi}}{V_{ref_{xp}}}$.

The basic flow belonging to this geometry is the fully developed flow which may be approximated for small values of the transverse curvature parameter ϵ_R as follows:

$$V_{Gx} \simeq \left(1 - y^2\right)\left(1 + \frac{1}{3}\epsilon_R y\right) + T_{wi}\left[\frac{1}{2}(1-y) + \epsilon_R \frac{1}{4}(y^2 - 1)\right] \qquad (1)$$

$$V_{G\varphi} \simeq S_{wa}\left[\frac{1}{2}(1+y) + \frac{\epsilon_R}{4}(1 - y^2)\right], \qquad (2)$$

where y is the radial co-ordinate with the origin shifted to the middle of the gap and normalised with H.

The equations governing small perturbations from this basic flow are obtainable in a straightforward manner by writing in the equations of motion in cylindrical coordinates (see eg. [11]) the velocity components and the pressure as a sum of the basic flow, $(V_{Gx}, 0, V_{G\varphi}, P_G)$, and perturbations, $(v_{sx}, v_{sr}, v_{s\varphi}, p_s)$, and neglecting squares of the latter. From this set of equations, the perturbation in pressure, p_s, may be eliminated by established procedures to derive the *Orr-Sommerfeld* and the *Squire* equations, see eg. [1], to yield a set of equations containing the velocity perturbations, $(v_{sx}, v_{sr}, v_{s\varphi})$ alone. The linearity of these resulting equations, together with the prevalent geometrical constraints, suggests solutions for the small perturbations to be sought in the form of waves propagating in the $x-$ and $\varphi-$ directions with wavenumbers λ_x and n_φ in the axial and azimuthal directions respectively, viz.

$$(v_{sx}, v_{sr}, v_{s\varphi}) = (A_{sx}, A_{sr}, A_{s\varphi}) exp^{i(\lambda_x x + n_\varphi \varphi - \omega t)} + c.c., \tag{3}$$

where $(A_{sx}, A_{sr}, A_{s\varphi})$ are complex and are functions of only the coordinate normal to the wall. The resulting set of ordinary differential equations for these complex amplitude functions which we wish to refer to in this order as the *extended Orr-Sommerfeld, Squire* and *continuity* equations respectively, forms the starting point for our study. These are as follows:

Extended Orr-Sommerfeld equation

$$\begin{aligned}
&\frac{d^4 A_{sr}}{dy^4}\left[\frac{1}{Re}\right] + \frac{d^3 A_{sr}}{dy^3}\left[\frac{2\epsilon_R}{Re}\right] \\
&+\frac{d^2 A_{sr}}{dy^2}\left[-\frac{2\lambda_x^2}{Re} + i\omega - i\lambda_x V_{Gx} - i\epsilon_r n_\varphi V_{G\varphi}\right] \\
&+\frac{dA_{sr}}{dy}\epsilon_R\left[-\frac{2\lambda_x^2}{Re} + i\omega - i\lambda_x V_{Gx}\right] \\
&-A_{sr}\left[\lambda_x^2\left(-\frac{\lambda_x^2}{Re} + i\omega - i\lambda_x V_{Gx} - i\epsilon_r n_\varphi V_{G\varphi}\right)\right. \\
&\left.-i\lambda_x\frac{d^2 V_{Gx}}{dy^2} + i\epsilon_R\lambda_x\frac{dV_{Gx}}{dy} - i\epsilon_R n_\varphi\frac{d^2 V_{G\varphi}}{dy^2}\right] \\
&-A_{s\varphi}\left[2\epsilon_R n_\varphi \lambda_x^2 V_{G\varphi}\right] = 0
\end{aligned} \tag{4}$$

Extended Squire equation

$$
\begin{aligned}
&A_{sr}\left[i\epsilon_R n_\varphi \frac{dV_{Gx}}{dy} - i\lambda_x \frac{dV_{G\varphi}}{dy} - i\epsilon_R \lambda_x V_{G\varphi}\right] \\
&+\frac{d^2 A_{s\varphi}}{dy^2}\left[\frac{i\lambda_x}{Re}\right] + \frac{dA_{s\varphi}}{dy}\left[\frac{i\epsilon_R \lambda_x}{Re}\right] \\
&+A_{s\varphi} i\lambda_x \left[-\frac{\lambda_x^2}{Re} + i\omega - i\lambda_x V_{Gx} - i\epsilon_r n_\varphi V_{G\varphi}\right] \\
&-\frac{d^2 A_{sx}}{dy^2}\left[\frac{i\epsilon_R n_\varphi}{Re}\right] - A_{sx} i\epsilon_R n_\varphi \left[\frac{\lambda_x^2}{Re} + i\omega - i\lambda_x V_{Gx}\right] \\
&+A_{sr}\left[i\epsilon_R n_\varphi \frac{dV_{Gx}}{dy} - i\lambda_x \frac{dV_{G\varphi}}{dy} - i\epsilon_R \lambda_x V_{G\varphi}\right] = 0
\end{aligned} \tag{5}
$$

Continuity equation extended to include transverse curvature

$$
\frac{dA_{sr}}{dy} + A_{sr}\epsilon_R + A_{s\varphi} i\epsilon_R n_\varphi + A_{sx} i\lambda_x = 0 \tag{6}
$$

It should be noted that V_{Gx} and $V_{G\varphi}$ in the equations (4, 5) are given by the equations (1, 2) which show the dependence of these quantities on the parameters for transverse curvature, swirl and axial velocity of the inner cylinder, viz. ϵ_R, S_{wa} and T_{wi} respectively. It is straightforward to verify that in the absence of transverse curvature and swirl, i.e. $\epsilon - R = 0$ and $S = 0$, the equations (4, 5, 6) reduce to the standard forms of these equations known in the literature, eg. [11]. The set of equations (4, 5, 6), together with homogeneous boundary conditions, define an eigenvalue problem, the dispersion relationship of which may formally be written as follows:

$$
F(Re, S_{wa}, T_{wi}, \lambda_x, n_\varphi, \omega) = 0. \tag{7}
$$

In the temporal eigenvalue problem, which is both convenient and sufficient for the purposes of this paper, λ_x and n_φ maybe considered real and ω permitted to be complex. For a neutraly stable disturbance the imaginary part of ω, denoted ω_i is zero.

3 The critical layer in the problem

Analogous to the classical shear flow stability problem, the *extended Orr-Sommerfeld equation* (4) exhibits a turning point for values of λ_x and n_φ for which the disturbance is neutrally stable. While there are similarities

between the turning points that appear in the classical problem and in the present one, there are also some noteworthy differences, and we focus our attention in this paper on the similarities and differences between the two.

3.1 Criterium for the location of the critical layer

In the classical problem ($\epsilon_R = 0, S_{wa} = 0$), the critical layer is located at the turning point, at which the coefficient of the second derivative, $\frac{d^2 A_{sr}}{dy^2}$, passes through zero for $Re = \infty$. This may be identified as the location where the phase speed of the neutrally stable wave, which is $\frac{\omega_r}{\lambda_x}$, is equal to the local velocity of the basic flow. This criterion needs modification when, as it is in the present problem, swirl is present in the basic flow.

The turning point of the *extended Orr-Sommerfeld equation* is located, as in the classical problem, where the coefficient of the second derivative for $Re = \infty$ is zero, which, from equation (4) is seen to be

$$[i\omega - i\lambda_x V_{Gx} - i\epsilon_r n_\varphi V_{G\varphi}] = 0 \tag{8}$$

An examination of the above equation (8) sheds light on the salient differences between the classical problem and the present one. Two kinds of source causing these differences may be identified, viz. transverse curvature and swirl. The differences, which are not just quantitative but already qualitative in nature, are as follows, whereby the observations are applicable, as in the classical problem, to neutrally stable disturbances:

- The location of the critical layer is affected by the transverse curvature in the geometry even in the absence of swirl since V_{Gx} depends upon ϵ_R, cf. equation (1). In this case, since transverse curvature destroys the symmetry of the axial velocity profile of the basic flow around the middle of the gap, see equation (1), the critical layer may not be expected to be located at the same distance from both the walls. Results of numerical computations to be presented later in the course of this paper will be seen to support this conjecture.

- When swirl is present, the axisymmetric mode of the disturbance, for which $n_\varphi = 0$, has no influence on the location of the critical layer. However, for all disturbance modes with $n_\varphi \neq 0$, the location of the critical layer is influenced by the azimuthal velocity profile of the basic flow, $V_{G\varphi}$.

- Furthermore, for the modes $n_\varphi \neq 0$, the critical layer is located not at the point where the phase speed of the wave is equal to the local

basic flow velocity, but where the frequency of the (neutrally stable) wave, ω_r, is equal to a quantity related to the inner product of the wave-number vector, (λ_x, n_φ) and the basic flow vector $(V_{Gx}, V_{G\varphi})$ and into which the transverse curvature in the geometry also enters, cf. equation (8). In view of the inherently vectorial nature of the basic flow velocity and the wave-number associated with swirl, it appears more meaningful to think in terms of the *slowness vector* introduced by Whitham [13] with components $(\frac{\lambda_x}{\omega_r}, \frac{n_\varphi}{\omega_r})$ instead of the phase speed of the wave, $\frac{\omega_r}{\lambda_x}$, that is customary in the classical problem.

3.2 Scaling property of the critical layer

The role of the critical layer in the context of flow transition, which is a subject with a long-standing tradition in fluid-mechanics research, see eg. [6, 10], has been discussed extensively and may be found in standard literature on this subject. For the present problem, the methods developed for studies in hydrodynamic stability are applicable, so we restrict ourselves to outlining the procedure and merely give a selection of some results.

The basic underlying idea is as follows:

Since the singularity at the turning point occurs only in the inviscid problem when the Reynolds number is set to infinity, viscosity may be expected to be effective only in the narrow regions surrounding the turning point, smearing out the large gradients. The mathematical procedure for treating such problems essentially consists of expanding the coefficients in the equations in a series around the turning point and rescaling such that the highest order derivatives which are traceable to effects of viscosity, are retained locally in the problem, see eg. [3, 4, 9].

Accordingly, we approximate the velocity components $V_{Gx}, V_{G\varphi}$ and its derivatives through series expansions around the turning point $y = y_c$ and write:

$$V_{Gx} = V_{Gx}(y_c) + V'_{Gx}(y_c)(y - y_c), V_{G\varphi} = V_{G\varphi}(y_c) + V'_{G\varphi}(y_c)(y - y_c), \quad (9)$$

and similarly for the derivatives of V_{Gx} and $V_{G\varphi}$. We scale the independent variable in the region $y = y_c$ as follows:

$$\frac{y - y_c}{\epsilon_c} = \eta_c, \quad (10)$$

where ϵ_c depends upon the Reynolds number Re in a manner to be determined. We may write $\epsilon_c = Re^{-n_{cd}}$ where n_{cd} belongs to the set of positive rational numbers. ϵ_c therefore tends to zero as the Reynolds number tends

to infinity, making η_c a suitable variable to describe large changes in narrow regions which is what the critical layer is. Writing the *extended Orr-Sommerfeld equation* (4) in terms of the rescaled variable η_c according to the equation (10), using therein the approximations (9), and examining the value of n_{cd} that retains the highest order derivatives (viscous terms) in the limit $Re \to \infty$ leads to $n_{cd} = \frac{1}{3}$ which means

$$\epsilon_c = Re^{-\frac{1}{3}}. \tag{11}$$

The equation (11) then gives the scaling of the critical layer. This is seen to be the same as in the classical problem. It can be used to derive approximations of the set of equations (4, 5, 6) valid in the critical layer and matching into the surroundings.

4 Numerical results

The eigenvalue problem defined through the differential equations (4, 5, 6) together with homogeneous boundary conditions was cast into an algebraic form through the spectral collocation method and solved numerically by the QZ-algorithm. The program was written in MATLAB for this purpose. We present a sample selection of results in this papaer.

Fig. 2 shows the axial and azimuthal velocity profiles in the basic flow for $\epsilon = 0.5, T_{wi} = 0.5$ and $S_{wa} = 0.5$. Figs.3 and 4 show plots of the amplitude functions of the disturbance at the critical Reynolds number for swirl-free and swirling annular flow.

Fig.5 is a sketch of the location of the critical layers in the class of flows under study. Figs. 6 and 7 are plots of the location of the critical layers close to the outer and the inner cylinder wall respectively ascertained from the numerical results according to (8). Figs. 8 and are plots of the amplitude and phase of the disturbance within these critical layers. We wish to draw the reader‘s attention to the different ways in which the location of the critical layers close to the outer and the inner cylinder walls are affected by the parameters T_{wi} and S_{wa}, figs.6 and 7.

References

[1] P.G.Drazin and W.H.Reid, *Introduction to Hydrodynamic stability*, Cambridge University Press (1982).

[2] W.O.Criminale, T.L.Jackson and R.D.Joslin, *Theory and Computation in Hydrodynamic Stability*, Cambridge University Press (2003).

[3] E.J. Hinch, *Perturbation Methods*, Cambridge University Press (1991).

[4] M.H.Holmes,*Introduction to Perturbation Methods*, Springer (1995).

[5] J.Kevorkian and J.D.Cole, *Perturbation Methods in Applied Mathematics*, Springer (1981).

[6] C.C.Lin, *The theory of Hydrodynamic Stability*, Cambridge University Press (1966)

[7] S.A.Maslowe,"Critical layers in shear flows", *Annual Review of Fluid Mechanics*, **1**8, 105–132 (1986).

[8] A.H.Nayfeh, *Perturbation Methods*, Wiley (1973).

[9] R.E.O'Malley Jr., *Introduction to Singular Perturbations*, Academic Press (1974).

[10] L. Rosenhead (Ed.), *Laminar Boundary Layers*, Oxford University Press (1963)

[11] H. Schlichting and K. Gersten, *Boundary-Layer Theory*, Springer (20??).

[12] F.Verhulst, *Methods and Applications of Singular Perturbations*, Springer (2000).

[13] G.B.Whitham, *Linear and Nonlinear Waves*, Wiley (1974)

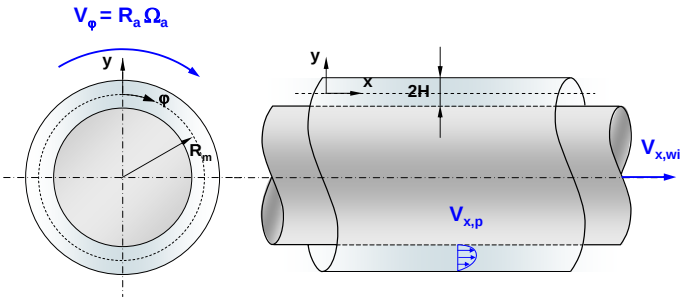

Figure 1: Sketch of flow geometry

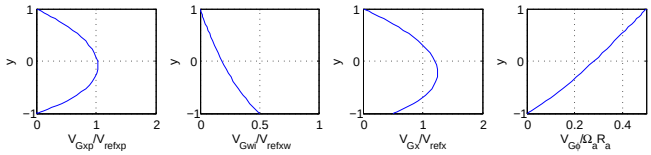

Figure 2: Axial and azimuthal velocity profiles in basic flow. $\epsilon_R = 0.5$, $T_{wi} = 0.5$, $S_{wa} = 0.5$

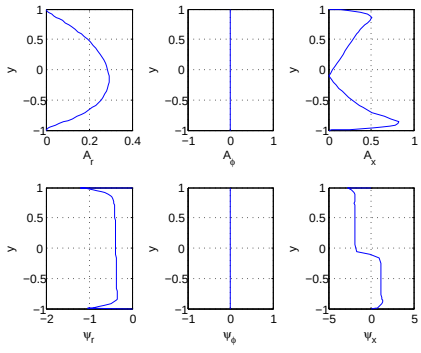

Figure 3: Amplitude functions for neutrally stable swirl-free annular flow. $Re = Re_{crit} = 7903$, $\epsilon_R = 0.1$, $T_{wi} = 0$, $S_{wa} = 0$, $\lambda_x = 0.2313$, $n_\varphi = 0$, $\omega_r = 0.2313$

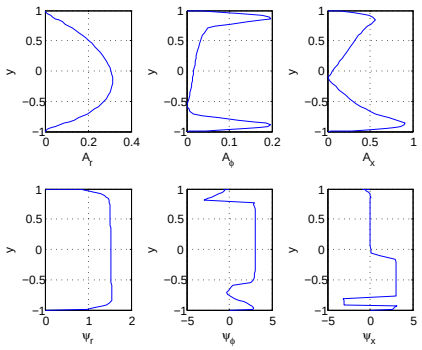

Figure 4: Amplitude functions for neutrally stable swirling annular flow. $Re = Re_{crit} = 7971$, $\epsilon_R = 0.1$, $T_{wi} = 0$, $S_{wa} = 0.01$, $\lambda_x = 0.9702$, $n_\varphi = 1$, $\omega_r = 0.2313$

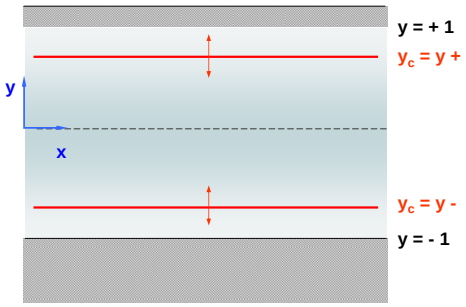

Figure 5: Sketch of annular flow showing location of critical layers

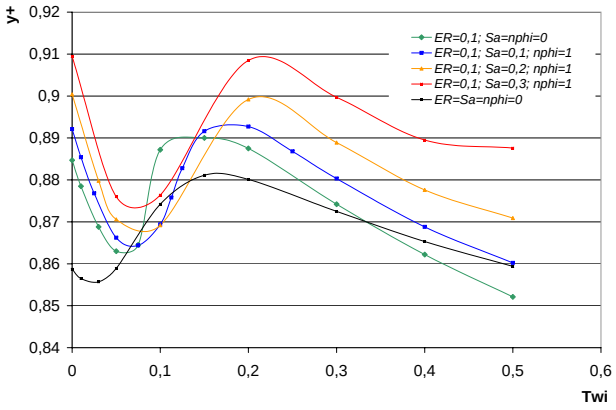

Figure 6: Effect of the translation and swirl parameters on the location of the critical layer close to the wall of the outer cylinder

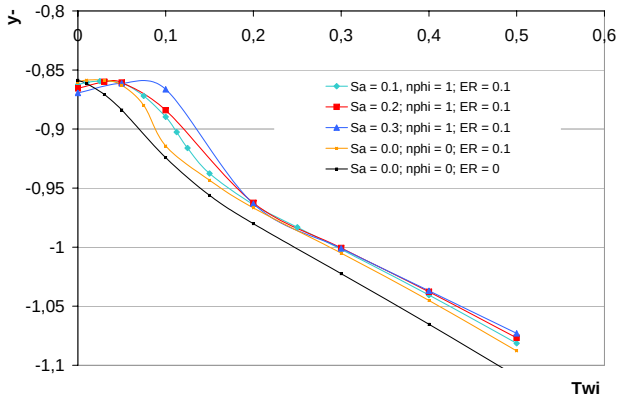

Figure 7: Effect of the translation and swirl parameters on the location of the critical layer close to the wall of the inner cylinder

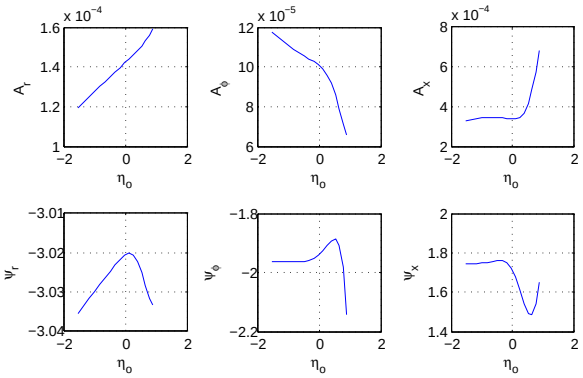

Figure 8: Distribution of amplitude and phase of the disturbance in the critical layer close to the wall of the outer cylinder

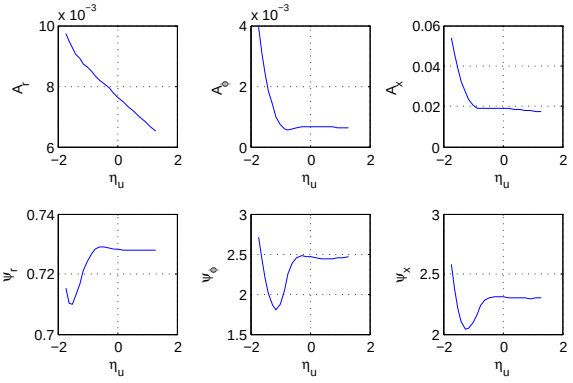

Figure 9: Distribution of amplitude and phase of the disturbance in the critical layer close to the wall of the inner cylinder